ELSEVIER

Biophysical Chemistry 91 (2001) 219–229

Biophysical Chemistry

www.elsevier.com/locate/bpc

Electrostatic effects on the free-energy balance in folding a ribosome-inactivating protein

Mark A. Olson*

Department of Cell Biology and Biochemistry, USAMRIID, 1425 Porter Street, Frederick, MD 21702, USA

Received 9 February 2001; received in revised form 30 April 2001; accepted 30 April 2001

Abstract

Electrostatics of globular proteins provides structural integrity as well as specificity of biological function. This dual role is particularly striking for ricin A-chain (RTA), an *N*-glycosidase which hydrolyzes a single adenine base from a conserved region of rRNA. The reported X-ray crystallographic structure of the RTA mutant E177A demonstrated a remarkable rescue of charge balance in the active site, achieved by the rotation of a second glutamic acid (Glu-208) into the vacated space. To understand this conformational reorganization, molecular-dynamics simulations were applied to estimate relative free energies that govern the thermodynamic stability of E177A together with mutants E177Q and E177D. The simulations anticipate that while E177A is a non-conservative substitution, the protein is more stable than the other two mutants. However, the structural plasticity of the RTA active site is not obtained penalty-free, rather E177A among the mutants shows the largest unfavorable net change in the electrostatic contribution to folding. Of the E177A folded state, reorganization of Glu-208 lowers the electrostatic cost of the free-energy change, yet interestingly, protein interactions oppose the rotational shift, while solvent effects favor the transition.

Keywords: Ricin A-chain; Thermodynamic integration; Molecular dynamics; Hydration

1. Introduction

Knowledge of the determinants that govern thermodynamic stability of globular proteins is essential for understanding structure–function correlates. For the large family of ribosome-inactivating proteins (RIPs), this includes factors that control the chain-folding process underlying translocation across cell membranes, as well as substrate recognition and binding to the ribosomal RNA. Upon cell uptake, RIPs function as *N*-glycosidases by removing an adenine base from 28S rRNA, consequently leading to inhibition of protein synthesis. Among the RIPs, ricin is the

* Tel.: +1-301-619-4236; fax: +1-301-619-2348.
E-mail address: molson@ncifcrf.gov (M.A. Olson).

0301-4622/01/$ - see front matter
PII: S0301-4622(01)00172-7

most cytotoxic [1,2]. Ricin is a heterodimer consisting of a 267-residue catalytic A-chain (RTA) linked by a disulfide bond to a 262-residue B-chain, which mediates endocytosis by binding galactose residues present on various cell-surface glycoproteins and glycolipids.

The X-ray crystal structures of ricin [3–5] and several mutants of RTA [6–8] reveal that the active-site cleft is balanced by a network of negative and positive charges. The core of the RTA molecule is a long connecting α-helix, which exhibits a distinct bend near its C-terminal end, allowing charged residues Glu-177 and Arg-180 to form an ion-pair interaction at the molecular surface of the active site (see Fig. 1). Both residues are invariant in all known RIPs and are thought to play crucial roles in the catalytic mechanism [9]. For substrate recognition and binding, there are seven additional highly conserved polar residues located in the active site and four flanking solvent-exposed positively charged residues.

Substitutions that alter the active-site charge balance lead to structural rearrangements of the active site plus decreases in solubility as a function of pH as compared to wild-type (WT) RTA [8]. One of the more interesting structures arises from the conversion of Glu-177 to alanine (E177A) [7]. This mutant shows a second glutamic acid proximal to Glu-177 rotated into the active site to replace the deleted side chain, thus presumably rescuing the charge balance of the WT structure. Catalytic activity is also remarkably rescued by the E177A mutant, showing an insignificant loss of 20-fold [10], whereas mutants E177D and E177Q exhibited activity losses of 80- and 180-fold, respectively [10,11]. Replacing Arg-180 with histidine affects the global stability of RTA if the imidazole ring is deprotonated [8].

It is well recognized that proteins in their native conformational state are in a delicate balance of protein and solvent forces which can be disrupted or stabilized by relatively small changes in the side chains of key amino acid residues. What is not clearly understood is how interactions among individual residues are integrated in providing structural 'plasticity'. To learn more about the factors that influence the stability of the RTA active site, molecular-dynamics (MD) simulations were carried out of the folded and unfolded (denatured) structures of three RTA mutants derived from Glu-177. Free-energy simulation methods using a finite-difference thermodynamic integration technique (reviewed by Kollman [12]) were applied to estimating the relative folding stability of mutants E177Q, E177D and E177A. Simulations of the folded states were initiated from the WT crystal structure and the unfolded states from an extended chain conformation. Free-energy differences were decomposed into contributions arising from protein and solvent interactions. Although free energies of denaturation have yet to be determined for RTA and the mutants, simulations presented here provide new insights into the electrostatics among active-site residues and water molecules. This is particularly important for predicting how a protein thought a priori to be both non-functional and less stable can rescue activity, as illustrated by the mutation E177A. A practical implication of establishing a predictive scheme for estimating the effects of structural reorganization is the structure-based design of protein mutations with modified rRNA binding specificity. The reported calculations extend previous theoretical studies of RTA bound with a 29-mer RNA hairpin and substrate analogues [13–15], which demonstrated binding determinants of significant electrostatic contacts, several of which mimic protein and solvent interactions predicted in stabilizing the native conformation.

2. Theory and computations

Free-energy differences for the folded and unfolded state of the enzyme (denoted as E) were calculated based on the following thermodynamic cycle:

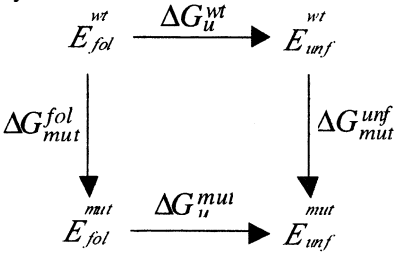

where ΔG_u^{wt} and ΔG_u^{mut} are the free energies of denaturation for the WT and mutant, respectively, and ΔG_{mut}^{unf} and ΔG_{mut}^{fol} are free energies for the unfolded and folded state, respectively, computed via simulation in which Glu-177 is converted to a substituting residue (Fig. 1). Substitutions studied include Glu → Gln, Asp and Asp → X and X → Ala, where X denotes an intermediate residue designed to eliminate the negative charge of Asp by replacing the carboxylate group with an aldehyde moiety. This latter residue retains both side-chain volume and hydrogen-bonding potential, and when combined with the other substitutions, permits a systematic determination of the structural conditions that allow charge-balance reorganization to take place in the active site. The relative free-energy change is obtained from the following:

$$\Delta\Delta G = \Delta G_u^{mut} - \Delta G_u^{wt} = \Delta G_{mut}^{unf} - \Delta G_{mut}^{fol}. \qquad (1)$$

The computational method employed in evaluating Eq. (1) is based on a finite-difference thermodynamic integration algorithm [12,16] in which the respective free-energy differences for the folded and unfolded state are calculated by using the following master equation

$$\Delta G = \int_0^1 \frac{\delta G(\lambda)}{\delta \lambda} d\lambda = \int_0^1 \left\langle \frac{\partial H(\lambda)}{\partial \lambda} \right\rangle_\lambda d\lambda, \qquad (2)$$

where the coupling parameter, λ, spans the interval from 0 (representing the WT state) to 1 (rep-

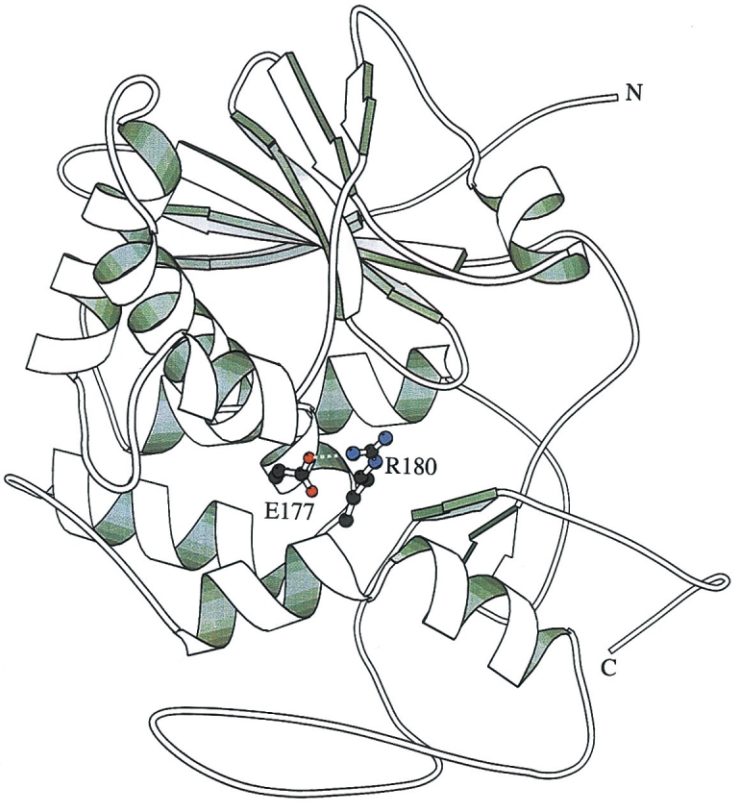

Fig. 1. Schematic illustration of a ricin A-chain Protein, highlighting the ion-pair interaction between residues Glu-177 and Arg-180. Figure produced using the MOLSCRIPT program [33].

resenting the mutant), and $\langle\ \rangle$ denotes an ensemble average over a Boltzmann sample of configurations governed by the Hamiltonian $H(\lambda)$. The kinetic component is generally not included in the free energy and the potential energy function $U(\lambda)$ is sampled. A statistical mechanical perturbation theory [17] can be used to compute $\delta G(\lambda)/\delta\lambda$ numerically by calculating the difference in free energy ΔG_i for a perturbation $\delta\lambda$ away from λ_i

$$\Delta G_i = -\frac{1}{\beta}\ln\langle e^{-\beta[U(\lambda_i \pm \delta\lambda) - U(\lambda_i)]}\rangle_{\lambda_i} \quad (3)$$

where $\beta = 1/k_B T$ (Boltzmann constant times absolute temperature). Calculations of Eq. (3) included both forward $(+\delta\lambda)$ and backward $(-\delta\lambda)$ perturbations with numerical integration of Eq. (2) carried out via a Gaussian–Legendre quadrature [18].

MD simulations were carried out for each λ point with trajectories generated for an active region composed of part of the enzyme inside a 12-Å spherical boundary centered on the initial position of Cβ of Glu-177 as derived from the X-ray crystal structure of the WT (PDB 1RTC). The unfolded state was represented as an extended conformation. Protein interaction potentials were modeled using the following form of the consistent valance force field [19]

$$\begin{aligned} U(\mathbf{R}) = & \sum_{\text{bonds}} K_b(b-b_0)^2 + \sum_{\text{angles}} K_a(\theta-\theta_0)^2 \\ & + \sum_{\text{dihedrals}} \frac{K_d}{2}[1+\cos(n\varphi-\gamma)] \\ & + \sum_{i<j}\left[\frac{A_{ij}}{r_{ij}^{12}} - \frac{B_{ij}}{r_{ij}^{6}}\right] + \sum_{i<j}\frac{q_i q_j}{\varepsilon r_{ij}} \\ & + \frac{1}{2}\sum_{i\in R} K_i \Delta r_i^2, \end{aligned} \quad (4)$$

where **R** denotes the set of all atomic coordinates specifying the system conformation, b_0 and θ_0 are the equilibrium bond length and angle parameters, respectively; K_b and K_a are the bond and bond-angle stretching constants, respectively; K_d is the torsional force constant; n is the periodicity of the torsional term, φ, and γ the phase angle; A_{ij} and B_{ij} are constants depending on the types of atoms i and j; r_{ij} is the distance separating atoms i and j, q_i (q_j) is the partial charge of atom i (j), ε is the effective dielectric constant; and K_i is the harmonic restoring force constant acting on atom i displaced Δr_i in boundary region R. Parameterization of Eq. (4) as a function of λ was implemented at the level of the force-field parameters; e.g. the first term is given by

$$\begin{aligned} U_{\text{bond}}(b;\lambda) = & [\lambda K_b(\lambda_B) + (1-\lambda)K_b(\lambda_A)] \\ & \times\{b - [\lambda b_0(\lambda_B) \\ & + (1-\lambda)b_0(\lambda_A)]\}^2 \end{aligned} \quad (5)$$

where λ_A and λ_B refers to the WT and mutant state, respectively.

Active regions were immersed in an 8–10 Å deformable layer of solvent water. Water was represented by the SPC force-field potential [20]. Ionization states for residues Asp, Glu, Lys, Arg and His correspond to a neutral pH. The active regions consisted of 64 residues (1063 protein atoms) and 370 water molecules for the folded structure, and eight residues (126 protein atoms) and 524 water molecules for the extended structure. Boundary regions contained 203 residues and seven residues for the folded and extended structures, respectively. Amino acid residues lying in unsolvated outer shells were kept harmonically restrained at their initial positions by employing a force constant corresponding to a positional mean-square fluctuation of 0.52 Å^2, determined via an average over all protein atoms in a full 0.5-ns MD simulation of the WT structure. Biasing the search of phase space was necessary, particularly for the unfolded form, where without restraints the volume of accessible microstates reflected highly flexible peptides, rather than a denatured protein structure.

The simulation protocol consisted of all systems simulated at 10 values of λ connecting the initial state to the mutated state. The λ_1 simulations were initiated with 400 cycles of minimization using the steepest descent algorithm plus 1000 cycles of minimization via a conjugate gradient algorithm followed by a 10-ps equilibration

phase. The initial atomic velocities were assigned from a Gaussian distribution corresponding to a temperature of 300 K. Simulations for λ_2, λ_3,..., λ_{10} were carried out after a 10-ps equilibration started from the final step of the previous simulation. Ensemble averages were determined from simulations of 60 ps per λ value with non-bonded interactions smoothed to zero beyond 11.0 Å and a constant dielectric constant ($\varepsilon = 1$) was used. End-point structures of the mutants ($\lambda = 1$) were determined following the λ_{10} simulation by averaging the trajectories of an additional 100-ps simulation. Integration of the equations of motion was performed using a 1.0-fs timestep.

3. Results and discussion

The free-energy simulation results for substitutions Glu-177 → Gln, Asp, and Asp → X and X → Ala are presented in Table 1. Supplementing the calculations of ΔG are free-energy decompositions at the protein (ΔG_{pro}) and solvent (ΔG_{sol}) level, with further decompositions at the force-field level. Since we are primarily interested in electrostatic interactions of the active site, van der Waals and covalent interactions are combined into a single non-electrostatic component. Decompositions derived directly from force-field interactions must invoke the caveat that their free-energy contributions depend on the particular integration path (see Boresch et al. [21] and references cited therein), as well as the choice of force field. By contrast, the overall free-energy difference between two end states is independent of the path connecting them. All decompositions are consistent with Eq. (2), with the gradient of the potential evaluated via a second-order finite-difference scheme.

The simulations show the mutants E177Q, E177D and E177A are destabilized by 2.0, 1.2 and 1.1 kcal/mol, respectively. Free-energy differences for E177A were calculated from adding the contributions of E177D, D177X and X177A. As discussed below, each net change in stability is due to the partial cancellation of many terms, both positive and negative, some of which stabilize the WT structure and others the mutants. These

Table 1
Changes in free energies (kcal/mol) for ricin A-chain mutants

Mutation	Free energy contribution	ΔG_{mut}^{unf}			ΔG_{mut}^{fol}			$\Delta\Delta G$		
		tot	ele	non-ele	tot	ele	non-ele	tot	ele	non-ele
E177Q	Total	69.3	62.6	6.7	71.3	62.2	9.1	−2.0	0.4	−2.4
	Protein	−9.4	−18.8	9.5	47.9	35.8	12.1	−57.3	−54.6	−2.7
	Solvent	78.7	81.4	−2.7	23.4	26.4	−3.0	55.3	55.0	0.3
E177D	Total	10.6	42.4	−31.8	11.8	43.5	−31.7	−1.2	−1.1	−0.1
	Protein	−6.4	30.4	−36.8	−21.7	12.8	−34.5	15.3	17.6	−2.3
	Solvent	17.0	12.0	5.0	33.5	30.7	2.8	−16.5	−18.7	2.2
D177X	Total	100.3	102.2	−1.9	101.8	103.6	−1.8	−1.5	−1.4	−0.1
	Protein	13.7	16.6	−2.9	74.7	76.4	−1.7	−61.0	−59.8	−1.2
	Solvent	86.6	85.6	1.0	27.1	27.2	−0.1	59.5	58.4	1.1
X177A	Total	−13.9	−1.3	−12.6	−15.5	−2.1	−13.4	1.6	0.8	0.8
	Protein	−8.5	7.1	−15.6	−9.7	3.6	−13.3	1.2	3.5	−2.3
	Solvent	−5.4	−8.4	3.0	−5.8	−5.7	−0.1	0.4	−2.7	3.1
E177A	Total	97.0	143.3	−46.3	98.1	145.0	−46.9	−1.1	−1.7	0.6
	Protein	−1.2	54.1	−55.3	43.3	92.8	−49.5	−44.5	−38.7	−5.8
	Solvent	98.2	89.2	9.0	54.8	52.2	2.6	43.4	37.0	6.4

findings are in accordance with the work of others [22–26] and would seem to underscore the characterization suggested earlier by Karplus and coworkers [23], that essential elements of the thermodynamics that govern protein stability are 'hidden' in the net free-energy change, either measured or computed.

As with any application of free-energy simulation methods, there are various approximations underlying the simulation model that can introduce errors in the calculations [26–28]. These include approximations due to the force fields, truncation of long-range forces, sphere radius of the active-site region, and computational sampling of phase space. Additional approximation is that the unfolded state lacks any residual secondary structure, although several experimental and theoretical works may disfavor this assumption. Requisite testing of the cutoff distance and sphere size used in the models, as well as the length of 700 ps for the MD simulations, suggest that they were adequate. Systematic errors were estimated from analyzing the hysteresis derived via forward and backward perturbations, and showed values of approximately ± 0.6 kcal/mol for each net ΔG determination.

3.1. Mutation Glu-177 → Gln

The individual free-energy changes from the amide substitution reflect predominately electrostatic components and show large unfavorable contributions, with values of 62.6 kcal/mol for the unfolded state and 62.2 kcal/mol for the folded state. The net effect on $\Delta\Delta G$ from electrostatic interactions is to marginally stabilize E177Q by 0.4 kcal/mol. Destabilization arises from non-electrostatic terms for a loss of -2.4 kcal/mol. Of the total $\Delta\Delta G$, electrostatic interactions from the protein are found to stabilize the unfolded chain conformation and destabilize the folded form, yielding a net decrease in stability of -54.6 kcal/mol. This loss is offset by a favorable electrostatic desolvation free energy of glutamine vs. glutamate, contributing 55.0 kcal/mol toward $\Delta\Delta G$.

The average MD simulation results for the active site of the WT structure and E177Q are illustrated in Fig. 2a,b. Overall, the modeled WT structure is in good agreement with the crystallographic determination reported by Robertus and coworkers [3]. The carboxylate of Glu-177 is anchored in place by an ion-pair interaction between Oε2 and Arg-180 NH_2, and a strong hydrogen bond between Oε1 and the hydroxyl of Tyr-123. The charge neutralization arising from E177Q alters both interactions. Moreover, the perturbation leads to unfavorable changes in hydration surrounding the active site. Three hydrogen bonds with water are calculated for the WT Glu-177; Oε1 bonds to two bridge forming waters, one forming a bridge to NH_2 of Arg-180 (similar to the water denoted as no. 334 of the crystal structure), and a second with Oε2 of Glu-208; Oε2 is hydrogen bonded to an additional third water. The simulation structure of E177Q shows one weak binding water molecule interacting with the side chain of Gln-177.

3.2. Mutation Glu-177 → Asp

Eliminating one methylene group from the side chain of Glu-177 yields a mutant E177D that is less stable by 1.2 kcal/mol than the WT structure, but 0.8 kcal/mol more stable than E177Q. In contrast with E177Q, the net electrostatic effect of the mutation is to favor the unfolded state ($\Delta\Delta G = -1.1$ kcal/mol). A further difference with E177Q is that the net protein electrostatic contribution for E177D favors the mutant form, while solvent effects destabilize the substitution. Of the folded conformation, the electrostatic perturbation on protein interactions is much less than the amide conversion (~ 13 vs. 36 kcal/mol). Fig. 2c shows the carboxylate of Asp-177 preserving the ion-pair interaction with NH_2 of Arg-180, although at an energetic cost of shifting the positively charged residue. Similarly, a hydrogen bond is formed comparable to the WT structure with the hydroxyl of Tyr-123, yet requires a conformational displacement of ~ 1 Å. Because the substitution conserves the negative charge, the carboxylate of Glu-208 is predicted to occupy a position similar to that of the WT structure, maintaining the interaction with Gln-173.

The simulation structure of the active-site re-

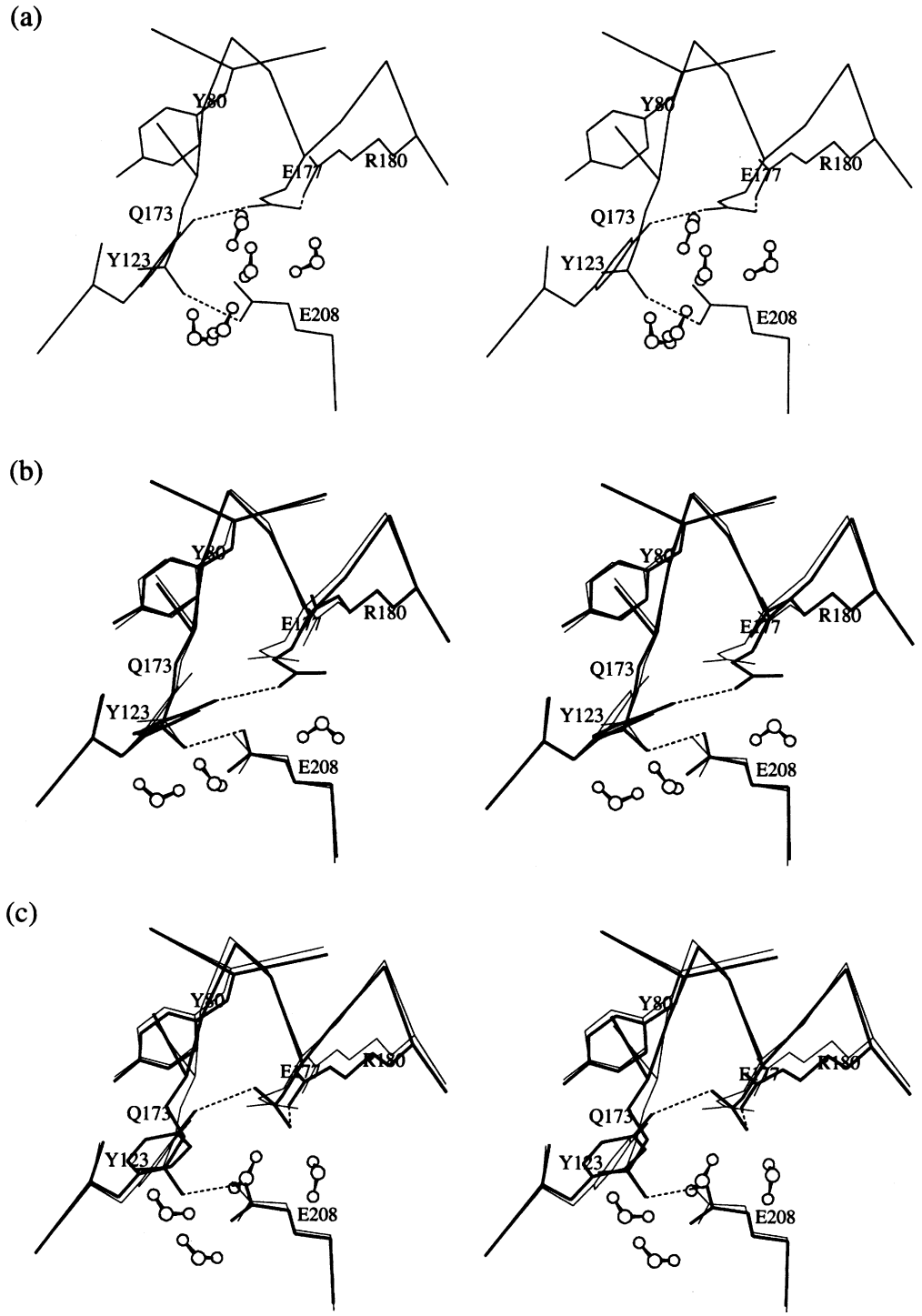

Fig. 2. Results of the molecular dynamics simulations of wild-type structure and amino acid substitutions at position 177 of the ricin A-chain protein in explicit solvent water. (a) The active site of the wild-type structure. Water molecules are illustrated as ball-and-stick models. Only the water interacting with side chains of Glu-177 and Glu-208 are shown. (b) Contrast between the calculated E177Q active site and the average simulation wild-type structure. The thick line denotes the mutant and thin line shows the wild-type protein. Waters correspond to the mutant structure. Simulation structures for (c) E177D and (d) E177A mutants.

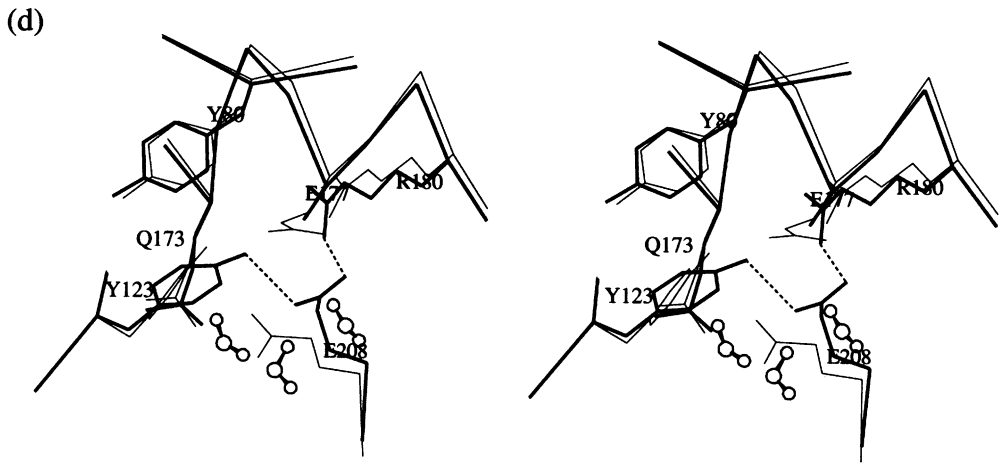

Fig. 2. (Continued).

gion indicates two waters are bound by Asp-177 and, because of the structural reorganization in residues Tyr-123 and Arg-180, the solvent contribution is less favorable than that calculated for E177Q. Nevertheless, the bound waters are more consistent with the WT structure and should contribute favorably to catalysis. For the unfolded state, displacement of the charge yields a more stable free energy of solvation than that corresponding to the charge deletion of E177Q.

3.3. Mutation Glu-177 → Ala

The free-energy perturbation of glutamate to alanine was expanded into three intermediate steps: E177D; D177X; and X177A. As mentioned above, X denotes a side chain in which the carboxylate of Asp has been replaced with an aldehyde group. The idea was to design a residue that eliminates the forking interactions of the carboxylate while retaining the potential for a single hydrogen bond. From Table 1, the conversion of Asp to X significantly disrupts the electrostatic stability ($\Delta\Delta G = -1.4$ kcal/mol) greater than either E177Q ($+0.4$ kcal/mol) or E177D (-1.1 kcal/mol). Protein contributions are unfavorable in both unfolded and folded conformations, leading to a net destabilization of -61.0 kcal/mol. The calculations for the folded form show that the decreased polarity for hydrogen bonding of X contributes to an electrostatic free-energy loss of nearly 30 kcal/mol greater than the charge neutralization of E177Q, and approximately 60 kcal/mol for a comparison with E177D.

Structurally, the residue X-177 preserves the hydrogen bond with Arg-180 (data not shown), although much weaker than the WT ion pair. The substitution also disrupts the electrostatic attraction between X-177 and Tyr-123. For residue Glu-208, the calculated structure indicates a lack of significant dihedral angle perturbation. This implies that the reduced solvent-exposed polarity at position 177 while retaining side-chain volume is insufficient to allow the proximal glutamate to reorganize the charge balance of the active site. As for solvent effects, the net contribution of transferring the mutant from vacuum to solution is favorable (~ 60 kcal/mol) and is similar to E177Q (~ 55 kcal/mol).

The replacement of X with alanine is the final step in obtaining E177A and yields a protein X177A that shows an *increase* in thermodynamic stability by a $\Delta\Delta G$ of 1.6 kcal/mol. The significance of this result is that the improved stability is obtained by the dihedral rotation of Glu-208 to fill the active-site cavity. The recovery in stability yields the least unfavorable electrostatic component among the series of folded protein changes arising from the substitutions. Moreover, the modification displays favorable net protein and

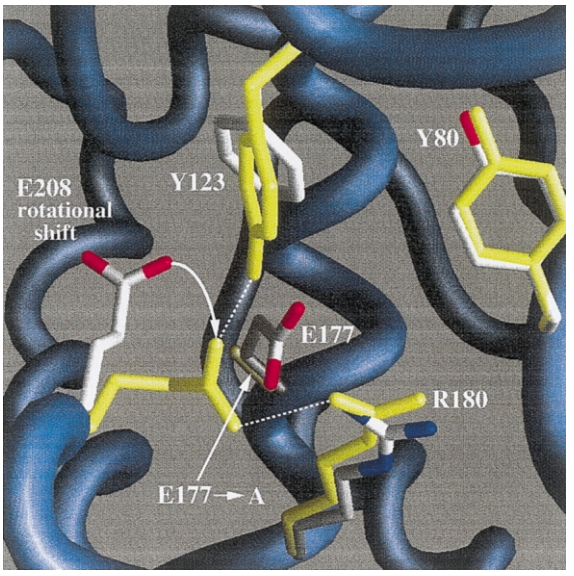

Fig. 3. Molecular modeling drawing of the reorganization calculated for the E177A structure and its comparison with the wild-type structure for ricin A-chain. The color yellow designates the side chains of E177A and the blue colored worm shows the backbone. Side chains of the wild-type structure are shown in white, with oxygen atoms illustrated in red and nitrogen atoms in blue. Figure produced using the GRASP program [34].

solvent contributions for both unfolded and folded conformations, however, the total electrostatic component from solvent interactions is unstable.

For E177A, individual contributions to $\Delta\Delta G$ are dominated by unfavorable electrostatic changes, yet interestingly, it is the non-electrostatic component that makes E177A more stable than either E177Q or E177D. The average simulation structure for the active site of mutant E177A is shown in Fig. 2d with a superposition of WT simulation structure and the two structures are contrasted schematically in Fig. 3. The structural difference is primarily the rotation of the carboxylate of Glu-208 in accordance with the X-ray crystal structure [7]. As expected, Ala-177 has no strongly interacting waters in the folded state and only one in the unfolded state through backbone interactions. Presumably, the functional hydration sites for catalysis are now provided by the side-chain reorganization in Glu-208.

From the average E177A simulation structure, the side chain of Glu-208 has dihedral angles of $\chi_1 = -140.2°$ and $\chi_2 = 62.5°$, which correspond to a less-populated rotameric state [29]. Because of the rotation, the carboxylate of 208 breaks the WT interaction with Gln-173, yet gains two alternative hydrogen bonds within the protein active site. The first is with Tyr-123, which undergoes a rearrangement allowing the interaction to take place, and the second is with the guanidinum group of Arg-180, which appears to move upward in the active site. The X-ray crystal structure of the mutant E177A also shows Tyr-80 rotated outward toward the solvent [7], whereas the simulation of 700 ps places the residue in a similar conformation as found in the WT structure. Owing to this lack of significant movement in Tyr-80 in the simulation, it is anticipated that the calculated $\Delta\Delta G$ of -1.1 kcal/mol may approximate an upper bound in stability change for E177A.

To understand better the role of Glu-208 and its rotation into the active site, additional free-energy simulations of X177 → A were preformed where the glutamate side chain was restricted to its WT configuration. The motivation for these calculations was a crystallographic analysis of the E177A structure, which showed that approximately 15% of the molecules retained the non-rotated configuration for Glu-208 [7]. Using occupancy populations of 85 and 15%, a free-energy difference between the two Glu-208 configurations is estimated at ~ -1 kcal/mol, favoring side-chain rotation. From the observation that the side-chain rotation of Glu-208 occurs during the X → A substitution, the simulation model for this perturbation provides a reasonable approach for calculating the conformational free-energy difference. Simulation results for the reorganization are presented in Table 2. Because of energy conservation problems with the WT configuration, thermal initialization was extended for both states to 75–80 ps per λ point starting with the λ_7 perturbation.

The results show that the side-chain reorganization in Glu-208 is favored thermodynamically by a ΔG of -1.4 kcal/mol. Without forcing the rotation in Tyr-80, the calculated ΔG is in excellent agreement with the crystallographic estimate. The calculations further show that the elec-

Table 2
Conformational reorganization free energy (kcal/mol) for residue Glu-208 in the structure E177A

Free energy contribution	ΔG			
	exp[a]	tot	ele	non-ele
Total	−1.0	−1.4	−0.5	−0.9
Protein	–	6.9	7.0	−0.1
Solvent	–	−8.3	−7.5	−0.8

[a] Experimental estimate taken from Kim et al. (1992).

trostatic component shifts the equilibrium between the two conformers toward structural reorganization. Moreover, and perhaps unexpected, the results indicate that relative to the WT configuration the protein interactions of the active site oppose the rotation of Glu-208. Despite the favorable pair-wise interactions of Glu-208 with side chains of Arg-180 and Tyr-123, electrostatic clashes with the residual protein backbone make ΔG_{pro} less than optimal. This is not to say that the reorganized protein free-energy surface is unfavorable, but rather the more populated E177A active-site configuration contains electrostatic strain. Conversely, solvent interaction promotes the conformational reorganization. The folding of E177A retains greater solvent accessibility for the side chain of Glu-208 than the WT configuration, and thus yields a lower desolvation cost reflected in the calculated electrostatic component of ΔG_{sol}. A similar argument can be suggested for Tyr-80 in the crystal structure, where side-chain rotation is favored due to solvent interactions.

From the model calculations, a general picture of the thermodynamic stability of the RTA active site emerges. While the electrostatic cost of desolvation due to the release of water from the protein active-site surface upon folding favors charge deletion of Glu-177, maintaining ion-pair complementarity is a necessary component for minimizing the thermodynamic loss in stability. This is evident from eliminating the negative charge at position 177 without allowing significant electrostatic reorganization (illustrated by mutants E177X or the WT configuration of E177A, both showing a value for $\Delta\Delta G \leq -2.5$ kcal/mol). Overall, structural plasticity arises from searching the free-energy surface for the configuration that yields the minimum reorganization penalty. Protein reorganization of RTA from charge deletions is unfavorable in terms of electrostatics, while solvent reorganization shifts the populations on the energy landscape in a fashion that recovers a significant fraction of the loss in conformational stability. Although still debated is the issue of whether hydrogen bonds make stabilizing contributions to the free-energy difference between the unfolded and folded state [30–32], it is clear that charge balance is a critical element of optimizing the self-organization of the native tertiary fold.

The calculations presented here demonstrate that free-energy simulation methods are capable of detecting a remarkable reorganization of the RTA active site subjected to the non-conservative perturbation of E177 → A. The E177A crystal structure emphasizes the importance of considering structural plasticity in interpreting mutagenic results. A promising aspect of the calculations is a modeling approach for understanding the underlying forces that stabilize RTA and its mutants. Moreover, the calculations provide a strategy for anticipating the effects of additional substitutions aimed at eliminating the cytotoxicity of ricin, while preserving antigenic determinants characteristic of the WT protein.

Acknowledgements

This work was supported by a generous grant of computer time from the Advanced Biomedical Computing Center of the Frederick Cancer Research and Development Center, National Cancer Institute.

References

[1] K. Eiklid, S. Olsnes, A. Pihl, Expt. Cell Res. 126 (1980) 321.
[2] S. Olsnes, A. Pihl, in: P. Cohen, S. van Heyningen (Eds.), Molecular Action of Toxins and Viruses, Elsevier Biomedical Press, New York, 1982, p. 52.

[3] B.J. Katzin, E.J. Collins, J.D. Robertus, Proteins 10 (1991) 251.
[4] E. Rutenber, B.J. Katzin, E.J. Collins et al., Proteins 10 (1991) 240.
[5] S.A. Weston, A.D. Tucker, D.R. Thatcher, D.J. Derbyshire, R.A. Pauptit, J. Mol. Biol. 244 (1994) 410.
[6] Y. Kim, J.D. Robertus, Protein Eng. 5 (1992) 775.
[7] Y. Kim, Y.D. Mlsna, A.F. Monzingo, M.P. Ready, A. Frankel, J.D. Robertus, Biochemistry 31 (1992) 3294.
[8] P.J. Day, S.R. Ernst, A.E. Frankel et al., Biochemistry 35 (1996) 11098.
[9] A.F. Monzingo, J.D. Robertus, J. Mol. Biol. 227 (1992) 1136.
[10] D. Schlossman, D. Withers, P. Welsh, A. Alexander, J.D. Robertus, A. Frankel, Mol. Cell Biol. 9 (1989) 5012.
[11] M.P. Ready, Y.S. Kim, J.D. Robertus, Proteins 10 (1991) 270.
[12] P. Kollman, Chem. Rev. 93 (1993) 2395.
[13] M.A. Olson, J.P. Scovill, D.C. Hack, J. Comput. Aided Mol. Des. 9 (1995) 226.
[14] M.A. Olson, Proteins 27 (1997) 80.
[15] M.A. Olson, L. Cuff, Biophys. J. 76 (1999) 28.
[16] W.F. van Gunsteren, in: W.F. van Gunsteren (Ed.), Computer Simulations of Biomolecular Systems, ESCOM, Leiden, 1989, p. 27.
[17] R.W. Zwanzig, J. Chem. Phys. 22 (1954) 1420.
[18] W.H. Press, B.P. Flannery, S.A. Teukolsky, W.T. Vetterling, Numerical Recipes in FORTRAN: The Art of Scientific Computing, Cambridge University Press, Cambridge, 1986.
[19] P. Dauber-Osguthorpe, V.A. Roberts, D.J. Osguthorpe, J. Wolff, M. Genest, T. Hagler, Proteins 4 (1988) 31.
[20] H.J.C. Berendsen, J.P.M. Postma, W.F. van Gunsteren, J. Hermans, in: B. Pullman (Ed.), Intermolecular Forces, Dordrecht, Reidel, 1981, p. 331.
[21] S. Boresch, G. Archontis, M. Karplus, Proteins 20 (1994) 25.
[22] L.X. Dang, K.M. Mertz, P.A. Kollman, J. Am. Chem. Soc. 111 (1989) 8505.
[23] J. Gao, K. Kuczera, B. Tidor, M. Karplus, Science 244 (1989) 1069.
[24] B. Tidor, M. Karplus, Biochemistry 30 (1991) 3217.
[25] T. Simonson, A.T. Brünger, Biochemistry 31 (1992) 8661.
[26] L. Wang, D.L. Veenstra, R.J. Radmer, P.A. Kollman, Proteins 32 (1998) 438.
[27] R.J. Radmer, P.A. Kollman, J. Comput. Chem. 18 (1997) 902.
[28] A. Di Nola, A.T. Brünger, J. Comput. Chem. 19 (1998) 1229.
[29] J.W. Ponder, F.M. Richards, J. Mol. Biol. 193 (1987) 775.
[30] Z.S. Hendsch, B. Tidor, Protein Sci. 3 (1994) 211.
[31] B. Honig, A.S. Yang, Adv. Protein Chem. 46 (1995) 27.
[32] J.K. Myers, C.N. Pace, Biophys. J. 71 (1996) 2033.
[33] P. Kraulis, J. Appl. Cryst. 24 (1991) 946.
[34] A. Nicholls, K.A. Sharp, B. Honig, Proteins 11 (1991) 281.